CHARACTERIZATION OF BIOMECHANICAL PROPERTIES OF ARTICULAR CARTILAGE USING MAGNETIC RESONANCE IMAGING

WONG CHIEN HING

This report is submitted
in fulfillment of the requirement for the degree of
Bachelor of Mechanical Engineering (Structure and Material)

Faculty of Mechanical Engineering

UNIVERSITI TEKNIKAL MALAYSIA MELAKA

MAY 2017

SUPERVISOR'S DECLARATION

I have checked this report and the report can now be submitted to JK-PSM to be delivered back to supervisor and to the second examiner.

Signature :.....

Name of Supervisor : DR. MOHD JUZAILA ABD LATIF

Date :.....

DECLARATION

I declare that this project report entitled “Characterization Of Biomechanical Properties Of Articular Cartilage Using Magnetic Resonance Imaging” is the result of my own work except as cited in the references

Signature : .....

Name : .....

Date : .....

ACKNOWLEDGEMENT

I would like to express my gratitude and appreciation to my supervisor, Dr. Juzaila Abd Latif who guide me to complete my final year project. His advice and guidance allow me to complete my report on time. Besides, I would also like to thank to my mentor, Ms Wana who had offered her help in the sample preparation and experiment for this final year project. Her advice was very helpful during the entire project. Furthermore, I would like to thank to my friends who always offered their idea and advice during the report writing as well as experiment. Lastly, I would like to express my deepest appreciation to my family who always support me during the four years of my degree program. With the advice and help from the particular mentioned, I am able to finish my final year report on time.

ABSTRACT

Osteoarthritis is a joint disease where the articular cartilage is degenerated slowly. Articular cartilage play an important role in reduce the friction between the bone and act as the shock absorber. Therefore, this study aim to characterize the biomechanical properties by using MRI technique and the combination of experimental and computational method. The used of MRI is to observe the cartilage surface and obtain the grayscale of the image. The experimental method in this study is indentation test whereas computational method is finite element (FE) modelling of articular cartilage. In this study, the bovine hip joint was used to study the biomechanical properties of articular cartilage. Indentation test is used to study the creep behavior and thickness of articular cartilage. For FE modelling, it is used to create a FE model of articular cartilage based on the real specimen to simulate the creep indentation test. By combining both experimental and computational method, the biomechanical properties, elastic modulus and permeability can be estimated. Moreover, a correlation between the grayscale value and biomechanical properties also been done. From this correlation, it can be shown that the grayscale value has a significant effect on the biomechanical properties of articular cartilage.

ABSTRAK

Osteoartritis adalah penyakit sendi di mana rawan artikular itu merosot perlahan-lahan. Rawan artikular memainkan peranan yang penting dalam mengurangkan geseran di antara tulang dan bertindak sebagai penyerap kejutan. Oleh itu, kajian ini bertujuan untuk mencirikan sifat-sifat biomekanik dengan menggunakan teknik MRI dan gabungan kaedah eksperimen dan pengiraan. Pengunaan MRI dalam kajian ini adalah untuk melihat permukaan rawan dan mendapatkan skala kelabu imej. Kaedah eksperimen dalam kajian ini adalah ujian lekukan manakala kaedah pengiraan adalah unsur terhingga (FE) model rawan artikular. Dalam kajian ini, hip sendi lembu telah digunakan untuk mengkaji sifat biomekanik artikular rawan. Ujian lekukan digunakan untuk mengkaji kelakuan rayapan dan ketebalan rawan artikular. Untuk pemodelan FE, ia digunakan untuk mewujudkan satu model FE rawan artikular berdasarkan spesimen sebenar untuk mensimulasikan ujian rayapan lekukan. Dengan menggabungkan kaedah kedua-dua eksperimen dan pengiraan, sifat-sifat biomekanik, modulus elastik dan kebolehtelapan boleh dianggarkan. Selain itu, hubungan antara nilai skala kelabu dan sifat biomekanik juga telah dilakukan. Dari hubungan ini, ia boleh ditunjukkan bahawa nilai skala kelabu mempunyai kesan yang besar ke atas sifat-sifat biomekanik artikular rawan.

CONTENT

LIST OF FIGURES

LIST OF TABLES

LIST OF ABBEREVATIONS

OA	Osteoarthritis
MRI	Magnetic resonance imaging
US	Ultrasound
OCT	Optical coherence tomography
ROI	Region of interest
BMI	Body mass index
ECM	Extracellular matrix
PG	Proteoglycans
FE	Finite element
PBS	Phosphate buffered saline
LVDT	Linear variable differential transformer

LIST OF APENDICES

CHAPTER 1

INTRODUCTION

1.1 BACKGROUND

Osteoarthritis (OA) is a joint disease, also called degenerative arthritis. This disease result from the breakdown of joint cartilage. In United State (US), studies on prevalence of osteoarthritis have presented that osteoarthritis affects 13.9% of adults (25 years old and above) and 33.6% aged over 65 years, with an approximate 27 million Americans suffer from OA (Chen et al., 2012). Besides, the women have higher chances being affected by the hand and knee osteoarthritis than men, especially in person age 50 years (Lawrence, et al., 2008).

OA is a degenerative joint disease where the articular cartilage (AC) has slowly worn away or breakdown. Articular cartilage is a white tissue that covers the end of the bone. The smooth surface of the articular cartilage reduce the friction occur in the human joint. There are many causes that result in the degeneration of articular cartilage, such as injury, overweight and others. The causes can be categorized into two types, which are traumatic mechanical destruction and progressive mechanical degeneration. The traumatic mechanical destruction happens because of abnormal or excessive use and injury of the joint whereas the progressive mechanical degeneration happen because of aging.

Knees, hips, neck, lower back, fingers joint and the bases of the thumb and big toe are often affected by OA. The patient that suffered from OA will feel the pain from the joint

whenever they move. This disease will affect their daily activity such as walking and exercising.

In previous study, many imaging methods are used to diagnose OA and observe the articular cartilage. Magnetic resonance imaging (MRI), ultrasound (US) and optical coherence tomography (OCT) are the additional approaches that have improved OA diagnosis and management through enhancement in the soft tissue depiction (Braun & Gold, 2012). Among all the imaging method, MRI is the best method for the assessment of articular cartilage due to its high contrast properties.

1.2 PROBLEM STATEMENT

MRI is the best technique available for evaluate the condition of articular cartilage since it has excellent soft tissue contrast (Eckstein et al., 2006).

In most of the previous studies, high-field MRI was used to analyze the in vivo precision of MRI-based volume and thickness measurement in patients with OA (Burgkart, et al., 2001; Kubakaddi, et al., 2013).However, the potential used of the low-field MRI has yet to be explore to assess the condition of articular cartilage. Furthermore, only geometrical studies were carried out to monitor the cartilage such as thickness, volume and joint space gap. Therefore, this study aimed to investigate the used of low field MRI in the characterization of biomechanical properties.

1.3 OBJECTIVES

The objectives of this study are as follows:

1. To characterize the grayscale of articular cartilage from the low-field MRI image.
2. To characterize the biomechanical properties of articular cartilage.
3. To correlate the MRI grayscale and biomechanical properties of articular cartilage.

1.4 SCOPE OF PROJECT

The scopes of this project are:

1. The sample used in this study is bovine hip joint.
2. The biomechanical properties are only concern on biphasic elastic modulus and permeability of articular cartilage.
3. The combination of experimental and computational method are used to characterize the biomechanical properties of articular cartilage.

CHAPTER 2

LITERATURE REVIEW

2.1 OSTEOARTHRITIS

Osteoarthritis (OA) is one of the chronic health disorders that affect the human normal life when they are aged. OA is caused by the degradation of articular cartilage. The breakdown of articular cartilage will limit the movement of human such as walking, running, even moving a finger will also cause some pain toward the OA patient.

OA represents a complex musculoskeletal disorder and is a form of disability. It ranks amongst the top five causes of disability (Chen et al., 2012). Other than that, OA does not only faced older people, but younger people will also have chances to endure this disease due to genetic problem or excessive burden on the articular cartilage. According to An Aging World: 2008, many countries in Asia are aging speedily. It is estimated that in year 2008 to 2040, the proportion of people aged 65 and above over in Singapore will increase by 316%, India by 274%, Malaysia by 269%, Bangladesh by 261% and Philippines by 256% (Kinsell & He, 2009). This has shown that with the increasing of aged people, people that will suffer from OA will also increase.

Although the OA affects all the joints in the human body, the hip and knees are the joints that usually affected by OA. In fact, OA causes more than 90% of the increasing number of total hip or knee joint replacement operations worldwide (Fransen, et al., 2011). Figure 2.1 shows the difference between normal knee and OA knee.

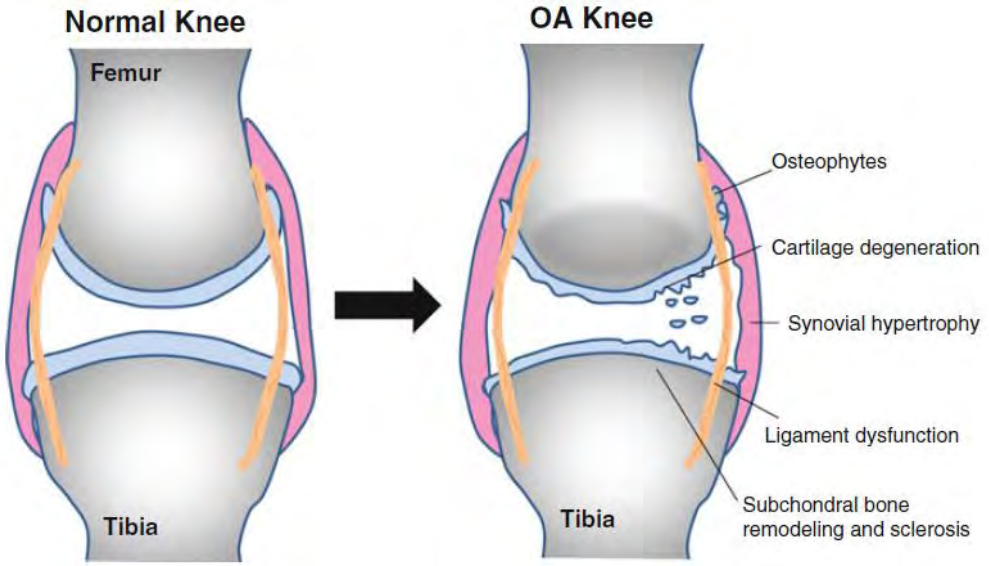

Figure 2.1: Schematic of normal vs. osteoarthritis knee joint (Kapoor & Mahomed, 2015).

2.1.1 Causes

There are some common causes for OA, such as injuries, degenerative of articular cartilage, disease and etc. The articular cartilage plays an important role in the movement that involve synovial joint, such as walking and running. Articular cartilage provides an almost frictionless sliding surface for the force to be transmitted during dynamic joint activity. When the surface of the articular cartilage is wear by the long term movement of the joint, degradation of articular cartilage will happen. This leads to the OA disease.

Aging is the main risk factor that causes OA. The biomechanical and biological changes as a result of aging are the contributing factor that causes degeneration of joint cartilage (Johnson & Hunter, 2014). Apart from aging, obesity is also a contributing risk factor for OA. A body mass index (BMI) larger than 30 kg/m^2 is considered obese, which is strongly related with knee and hand OA. Some of the metabolic and inflammatory system may affected by the people who is in obesity condition (Palazzo et al., 2016). Injuries and

overused of joint cartilage will also result in degeneration of articular cartilage. The individual with the occupation that heavily involve the knee joint double the risk of cultivating knee OA compare to the occupation that involve less physical activity (Messier, et al., 2009).

Compare to men, women has the higher risk to suffer from OA. According to Palazzo et al, women have the higher risk to suffer from knee, hip and hand OA compare to men, especially around menopause. According to study, at least 60 % of the hip and hand OA and up to 40 % of knee OA are due to genetic problem (Spector & MacGregor, 2004). While many studies focus on OA commonness, many genes have been recognized in playing a role in OA pathophysiologic pathways and thus may result to OA risk. Studies also had shown that many genes have been perceived to be related to OA.

2.1.2 Symptoms

The people who suffer from OA will have some sense of pain whenever they use their joint. Normal activity like walking, running, lifting something will also cause some pain to the OA patient. OA usually happen in hand, knee and hip. For hip OA, the groin area or buttocks will feel pain whenever the patient is moving around. Besides, there is some cracking sound when the OA patient bending their joint, such as finger and elbow. After some time or few years, these joint areas are getting swollen. The symptoms can be easily spotted through observed these joint areas. When finger and hand joint are affected by OA, some simple activities such as hold and grasp an object, writing or activities that involve using the joint will be difficult to carry out.

2.1.3 Diagnosis

For OA, there are two types of diagnosis, which are physical examination and diagnosis test. Physical examination is important in detecting OA. Each joint has unique physical examination finding (Sinusas, 2012). The testing of the range of movement and special function test such as ligament stability, meniscus and gait analysis are the basic analysis of OA (Michael et al., 2010).

Another method used to diagnose OA is by using imaging method. Plain radiography (X-Ray), Computed Tomography (CT Scan) and Magnetic Resonance Imaging (MRI) are commonly used to diagnose OA. Among these methods, MRI is able to provide more auspicious result in the assessment of cartilage status (Burgkart, et al., 2001). MRI provides an excellent soft tissue contrast and it is capable to differentiate different types of soft tissue in a joint (Soh, et al., 2014).

2.1.4 Treatments

OA is a disease that cannot be completely cured, but there are some medications to relieve the pain that OA patient suffered. Treatment for OA usually has four categories, which are non-pharmacologic, pharmacologic, complementary and alternative, and surgical (Sinusas, 2012). Non-pharmacologic often starts with physical activity. Physical activity is proven widely to decrease the pain of OA patient (Vignon, et al., 2006). According to Vignon, activities of daily life (ADL) such as housekeeping, shopping, do-it-yourself projects, gardening and recreational walking are some kind of physical activities that help in OA.

For pharmacologic treatment, Acetaminophen and non-steroidal anti-inflammatory drugs (NSAIDs) and Intra-articular steroid injections are the main treatment of OA (Taruc-Uy & Lynch, 2013). Besides, there are also some supplement for OA such as glucosamine

and chondroitin. The supplement such as glucosamine and chondroitin are effective for moderate to severe knee osteoarthritis (Sinusas, 2012).

Other than that, surgical treatment is also available for OA patient, but it is only reserved for patients whose symptoms have not responded to other treatment. Total joint replacement is an effective surgical intervention for OA treatment (Sinusas, 2012). Before surgical treatment, all OA patients should receive at least some treatment from the first two categories and go surgical treatment if only the first two categories have shown no effect.

2.2 ANATOMY OF SYNOVIAL JOINT

Synovial (diarthrodial) joints provide the body with the ability to maintain posture, and some simple movement such as walking and running. The synovial joint is covered by synovial membrane as shown in Figure 2.2. The synovial membrane release synovial fluid which acts as lubricant for the joint movement.

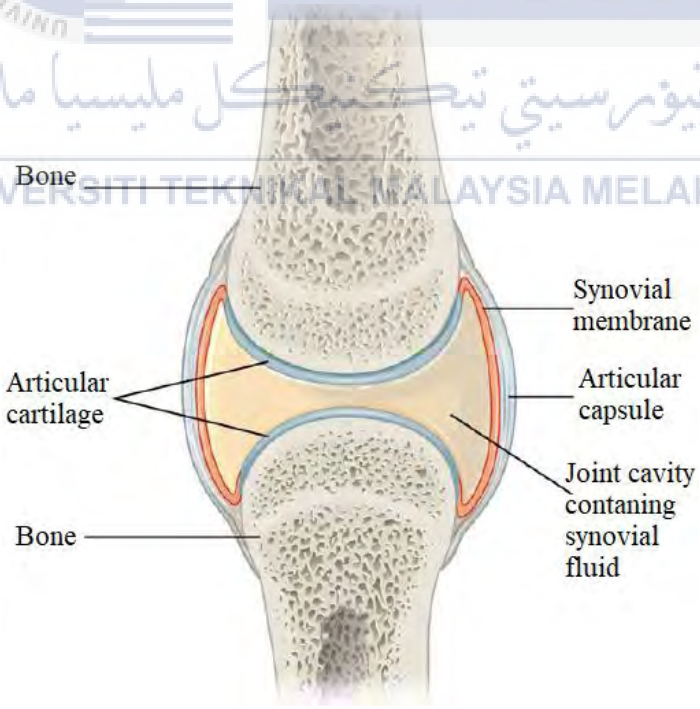

Figure 2.2: Structure of synovial joint (Heyden, 2016).

There are six types of synovial joints as shown in Figure 2.3. These include hinge, condyloid, saddle, pivot, plane, and ball and socket joint (Heyden, 2016).

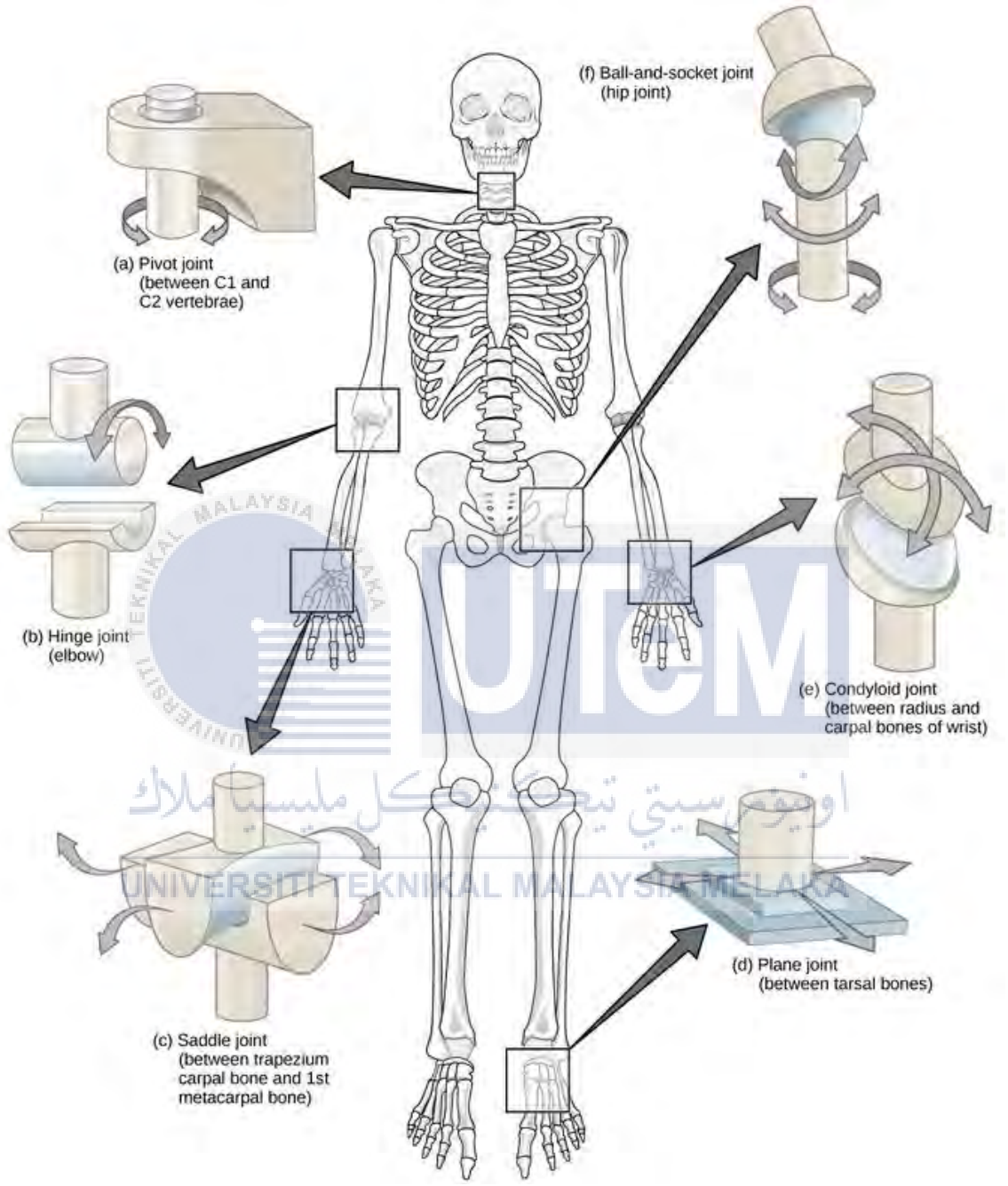

Figure 2.3: Types of synovial joint (Heyden, 2016).

Table 2.1: Description of each joint

Joint	Description	Example
Planar joint	Allow gliding movements; also called gliding joints. Not involve rotation and the range of motion is limited.	Carpals of the wrist, acromioclavicular joint
Hinge joint	Act as a door hinge, allowing flexion and extension in just one plane.	Elbow
Pivot joint	This joint allows rotational movement	Atlanto-axial joint, proximal radioulnar joint, and distal radioulnar joint.
Condyloid joint	Also called as ellipsoidal joint. Allows angular movement along two axes, such as joints of the wrist and fingers, which can move both side to side and up and down.	Wrist joint (radiocarpal joint)
Saddle joint	Allow angular movements similar to condyloid joints, but with a greater range of motion.	Thumb joint
Ball and socket joint	Allows the greatest range of motion, as all movement types are possible in all directions.	Shoulder and hip joints.

2.3 ARTICULAR CARTILAGE

Articular cartilage is a smooth and glistening bluish-white tissue that exist in synovial joint of human body. Articular cartilage covers the end of bones of a joint and it act as lubricant whenever the bones glide over each other with a small amount of friction.

2.3.1 Composition and Structure of Articular Cartilage

Articular cartilage is a biphasic material, which means that it consist of two phases, solid and fluid phase. The solid section is permeable and represented by solid matrix that consist of collagen fiber and proteoglycan molecules, and the fluid section is made up of extracellular water with dissolved ions and nutrients (Juras, et al., 2009). The thickness of articular cartilage is about 2 to 4 mm. Articular is a type of tissue that does not have blood vessels, nerves or lymphatic. It is composed of a dense extracellular matrix (ECM), which

composed of water, collagen and proteoglycans, with lesser amount of non-collagenous protein and glycoproteins, with a highly specialized cells called chondrocytes. All these compositions used to retain water within the ECM and it is critical to maintain its unique mechanical properties (Fox et al., 2009). The structure of articular cartilage consist of four zones as shown in Figure 2.4.

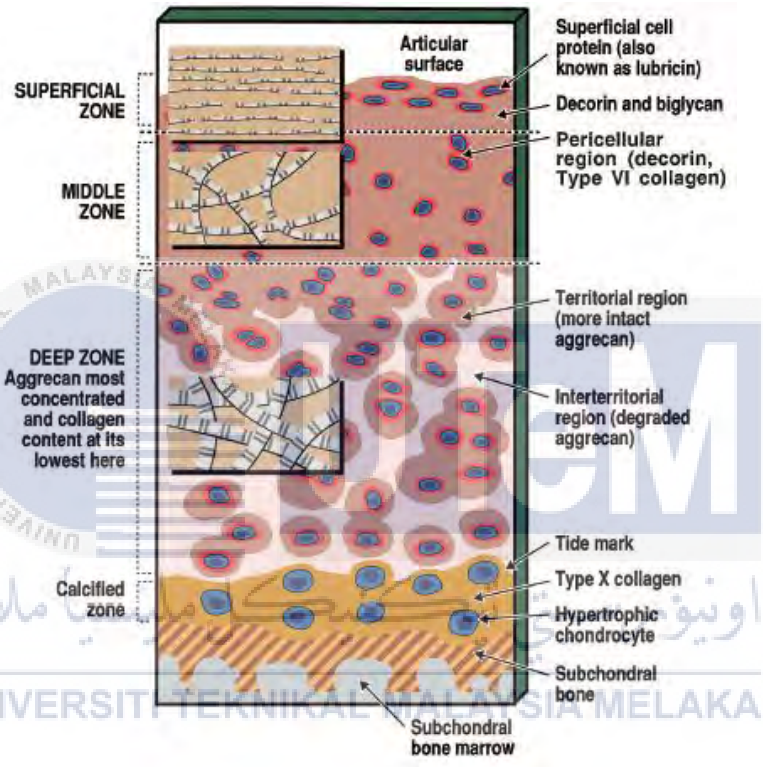

Figure 2.4: Diagrammatic representation of the general structure of human articular cartilage from an adult to show the zones, regions, and relationship with subchondral bone (Poole, et al., 2001).

In the superficial zone, the superficial cells are surrounded by thin collagen fibrils that generally run parallel to each other and to the articular surface. Due to the superficial zone provide the highest tensile properties, the articular cartilage has the ability to accommodate the shear, tensile and compressive forces encountered during articulation. The layer below superficial zone is midzone where the cell density is lower. It has the more

rounded cells and an extensive extracellular matrix rich in the proteoglycan aggrecan. In the deep zone, there is an interterritorial region distinguishable by the ultrastructure of aggregates of the proteoglycan.

Articular cartilage have the water contain of 60-80%, and the chondrocytes is surround by extracellular matrix (ECM). Inside the ECM, it composed of type II collagen (5-10% of total cartilage composition) and proteoglycans (PG) molecule (10-20%). The mechanical support of the articular cartilage is provided by these components (Hani, et al., 2011).

2.3.2 Function of Articular Cartilage

Articular cartilage provides a low friction, wear resistance surface to the joint and have a function to distribute stresses that faced by the bone. The inhomogeneity and anisotropy of the tissue's mechanical properties was resulted by the complex composition and the structure of cartilage (Wang, et al., 2002). This mechanical properties of articular cartilage make the cartilage to be nearly frictionless and absorb shock.

2.3.3 Biomechanical Properties

The mechanical response of articular cartilage is heavily tied to the fluid flow through the cartilage. The fluid flows across the articular surface when the articular cartilage is deformed. Acknowledging that the fluid flow and deformation are interdependent has led to the modeling of articular cartilage as a mixture of fluid and solid components (Mansour, 2009). This is known as the biphasic model of cartilage. In this biphasic material properties, all the solid-like components represent the solid phase of mixture, whereas the interstitial fluid is free to move through the matrix of fluid phase. For this biphasic behavior, the solid

phase assumed as an incompressible elastic material, and the fluid is assumed as an incompressible and inviscid (Mansour, 2009).

In articular cartilage, there are two important properties that play important role in its function, which are elastic modulus and permeability. To know how the articular cartilage function within its structure, it is important to know that the mechanical behavior (stress-strain) of the cartilage. The proportionality constant between stress and strain is known as elastic modulus and Poisson's ratio. Poisson's ratio represents the compressibility of the articular cartilage. A ratio of 0.5 illustrates an incompressible material, whereas a Poisson's ratio of 0 illustrates a highly compressible material (Lu & Mow, 2008). The fluid component within the tissue may flow out of the tissue when it is being compressed and this is the measure of its permeability. The low permeability indicates that it is harder to force the fluid to pass through the solid matrix. In articular cartilage, the solid phase is elastic and permeable to fluid.

From the previous study, human articular cartilage has a significant higher modulus which is 4.89 ± 0.76 MPa, compare to porcine and bovine cartilage, which are 1.18 ± 0.17 MPa and 1.86 ± 0.44 MPa respectively (Taylor, et al., 2011). It is also found that porcine articular cartilage was the most permeable ($6.33 \times 10^{-16} \pm 9.04 \times 10^{-17}$ m^4/Ns) compare to human ($1.96 \times 10^{-16} \pm 2.05 \times 10^{-16}$ m^4/Ns) and bovine ($2.70 \times 10^{-16} \pm 1.08 \times 10^{-16}$ m^4/Ns).

2.3.4 Thickness

The deformation of articular cartilage normally depend on the thickness of the articular cartilage. The thickness of articular cartilage is different from joint to joint. It seems to be related to the congruence of a joint. There is a significant relationship between the thickness of cartilage and pressure brought to bear on the joint surface (Simon, 1970). The cartilage of congruent joint such as the ankle is found to be thin, whereas the cartilage of incongruent joint such as knee is found to be thicker (Shepherd & Seedhom, 1999). The thickness of cartilage varies depending on species, age and the type of joint. Previous study has shown that the thickness of cartilage between human and animal is difference. The thickness of human cartilage was 1.82 ± 0.18 mm, bovine cartilage was 1.32 ± 0.13 mm thick, porcine cartilage was 1.22 ± 0.10 mm thick, and ovine cartilage was 0.52 ± 0.10 mm thick (Taylor, et al., 2011).

2.4 MAGNETIC RESONANCE IMAGING OF ARTICULAR CARTILAGE

MRI is one of the most important devices used to diagnose the condition of the articular cartilage since the discovery of X-ray. MRI use non-ionizing radio waves to induce a signal from paramagnetic nuclei tissue. Nowadays, MRI is used for the evaluation of articular cartilage due to its high soft-tissue contrast. Mostly conventional MRI sequences are commonly used to detect morphological changes by providing T_1, T_2, and spin density weighted images (Schrauth, et al., 2016). MRI techniques can determine many tissue parameters that are important to repair or transplant cartilage by obtaining the biomechanical and physiological information. Besides, MRI can also use to assess the cartilage thickness and volume (Goldy, et al., 2006).

Human body is make up of 80 % of water. MRI create magnetic field and make the proton from water molecules to align in it and make the proton spin. The strength of magnetic field depends on the radio frequency created from the MRI scanner. The proton absorb energy from the field and spin. A process called precession, which means that the proton slowly return to its normal spin. This process produce a radio signal that can be measured by the receiver in the MRI and convert it into an image (Mcmahon, et al., 2011). During the scanning, an echo is form to collect the signal and generate the transverse magnetization. The echo created is depends on the radio frequency and thus forming different MRI sequence, and thus create different contrast of MRI image.

MRI generally divided into low-field, high-field and ultra-high field MRI. The difference between low-field, high-field and ultra-high field MRI is their magnetic field. Magnetic field that below 0.3 Tesla (T) is consider as low-field MRI, 0.3T – 1.0T is mid field MRI, 1.0T – 7.0T is high-field MRI and above 7.0T is consider as ultra-high field MRI. Many research have compare the result between high field and low field. According to Magee, the image scan by high field MRI contribute better spatial and contrast resolution image than low field MRI (Magee, et al, 2003). In terms of costing, high field MRI is expensive and higher maintenance fees compare to low field MRI.

2.4.1 Studies of Articular cartilage using Low-field MRI

One of the study had utilize the use of low-field MRI to investigate the normal canine stifles and compare MRI image to gross dissection. A 0.2T MRI were used to analyze the synovial fluid and radiographic examination of stifle joint from 12 dogs (Pujol, et al., 2010). In this study, three sequences were used, T1-weighted spin echo in sagittal, coronal and transverse plane, T2-weighted spin echo in sagittal plane and T1-gradient echo in sagittal

plane. According to this study, low-field MRI protocol provide satisfactory image quality to assess the canine stifle joint.

2.5 METHOD TO CHARACTERIZE THE BIOMECHANICAL PROPERTIES ARTICULAR CARTILAGE

In previous study, both the experiment method and analytical solutions are commonly used to characterize these biphasic properties of the cartilage (Latif, et al., 2013). Yet, the indentation test is the most preferred in characterize the biomechanical properties of cartilage due to its test set-up can allow the cartilage to be immersed in the fluid during the test and the ease of sample preparation. The thickness test and creep test can carry out by using an indentation test. Instead of using only the single experiment method or analytical solutions, recent study had used the combination of indentation test and finite-element (FE) modelling to characterize the biphasic properties of articular cartilage (Katta, et al., 2007).

To characterize the biphasic properties of articular cartilage, a linear axi-symmetric biphasic poroelastic finite element (FE) model is generated to simulate the creep indentation test. This model was used to determine the elastic modulus and permeability of articular cartilage. These properties need to be sequentially tuning until the model output matched the indentation test results (Latif, et al, 2012). The model was generated by using Abaqus 6.9-1 (DS Simulia Corp., Providence, RI, USA). Both the creep indentation and thickness test result are used to derive the intrinsic material properties, which are elastic modulus and permeability. The finite element model is completed by using an axisymmetric biphasic poroelastic finite element (FE) modelling method. The predicted curve produced form the FE model is fit to the experimental curve. After the curve fitting process, the elastic modulus

and permeability are determined using MATLAB software and these result are taken as the actual mechanical properties of the articular cartilage (Taylor, et al., 2011).

2.6 SUMMARY

The use of low-field MRI can be used to study the articular cartilage of bovine articular cartilage as to achieve the objective in this study. Previous study had used MRI to analyze the volume and thickness measurement of articular cartilage. Therefore, in this study, the combination of experimental and computational method are used to estimate the biomechanical properties of articular cartilage as refer to the previous studies. The correlation between MRI grayscale also been made to show the relationship of MRI grayscale and biomechanical properties of articular cartilage.

CHAPTER 3

METHODOLOGY

3.1 INTRODUCTION

This chapter discusses about the equipment, materials, experimental methodologies and computational methodologies that used to characterize the biomechanical properties of articular cartilage. The experimental methodologies include sample preparation, MRI scanning, indentation test while computational methodologies include the finite element (FE) modelling of articular cartilage. The biomechanical properties of articular cartilage is determined by the combination of both methods. The flow chart of methodology was shown in Figure 3.1.

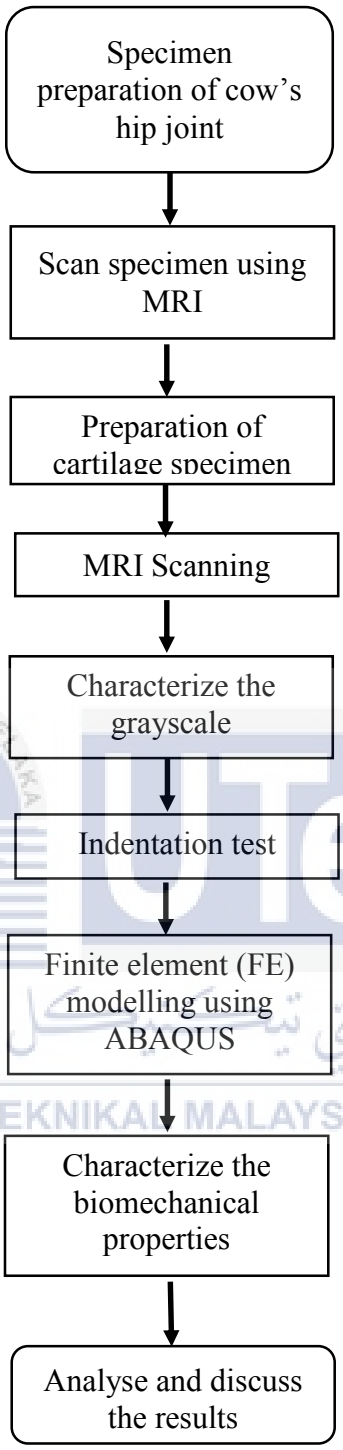

Figure 3.1: Flow chart of methodology

3.2 SPECIMEN PREPARATION

3.2.1 Phosphate Buffered Saline

Phosphate buffered saline (PBS) is a water-based salt solution that commonly used in biological research. In this study, PBS was used for irrigation purpose during the sample preparation procedure and also to equilibrate the cartilage during the indentation test (Latif, 2011). As the recommendation from the manufacturer (www.mpbio.com), it was prepared using a PBS tablet dissolved in sterile distilled water at the ratio of one tablet in 100 ml. The PBS tablets' composition was shown in Table 3.1.

Table 3.1: Formulation of the PBS tablets used in this study. Adapted from Latif (2011)

Component	Concentration (mg/L)	Molecular Weight (Da)	Molarity (mM)
Potassium Chloride (KCl)	200.0	74.55	2.68
Potassium Phosphate Monobasic (KH2PO4)	200.0	136.09	1.47
Sodium Chloride (NaCl)	8000.0	58.44	136.89
Sodium Phosphate Dibasic (Na2HPO4)	1150.0	141096	8.10

3.2.2 Cartilage Specimen Preparation

The bone is extracted from a slaughter cow and the part that extracted is an intact joint. By using an electric saw, the intact joint is cut into the size that can be fit into the MRI machine. After scanned by MRI machine, the femoral head of the intact joint is separated from the hold bone. After that, the femoral head is cut into four small pieces as shown in Figure 3.2 so that it can be fitted in the specimen holder. After the specimen is cut into four pieces, it is wrapped with tissue that soaked with PBS solution, then it is stored in the fridge

and tested within 24 hours. In this study, two sample were used and total number of specimens are eight (n = 8).

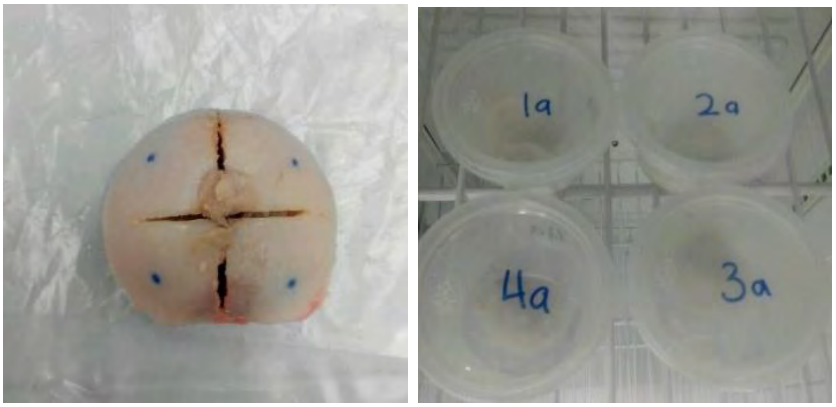

a. b.

Figure 3.2: Specimen preparation (first sample), a. Cow bone (femoral head). b. Four specimens wrapped with PBS tissue.

3.3 MAGNETIC RESONANCE IMAGING SCANNING

Before the specimen is cut into four small pieces, MRI scanning is carried out to measure the cartilage thickness and obtain the grayscale image. There are plenty of MRI sequences and different sequence give different contrast. Besides, there are three planes that used in scanning, which are sagittal, transverse and coronal plane for each sequence. In this study, five sequences are used, which are gradient echo (GE), gradient echo STIR (GE-STIR), spin echo T1 (SE-T1), spin echo T2 (SE-T2) and turbo spin echo (TSE). From these five sequences, the best sequence is chosen so that it can show the high contrast clear image and easy to determine the thickness and grayscale. The properties of each sequences are shown in Table 3.2.

Table 3.2: Properties of each sequence used in MRI scanning.

Sequences	Slices	Thickness between slices
Gradient echo	29	4.0 mm
Gradient echo STIR	29	4.0 mm
Spin echo T1	29	4.0 mm
Spin echo T2	29	4.0 mm
Turbo spin echo	29	4.0 mm

After the specimen is cut into four small specimens, these specimens were scanned again by using the highest contrast sequence and plane. This purpose was to characterize the grayscale.

The MRI scanned image is used to determine the grayscale value of the articular cartilage. The software used to determine the grayscale is MATLAB R2014a (MathWorks Inc., MA, USA). The image file scanned by MRI is imported to the MATLAB by input the suitable command. After import the image, the suitable region of interest (ROI) is cropped by using the suitable command. The grayscale value of each level is determined and the average grayscale is calculated. A low grayscale value is not considered in the calculation of average grayscale value. The grayscale value is used to characterize the biomechanical properties of articular cartilage. A bright colour shown in grayscale image means it has a high value of grayscale value. There are two layer grayscale layer, the outer layer represents the fluid phase of articular cartilage whereas inner layer represents the solid phase. The grayscale and its crop image are shown in Figure 3.3.

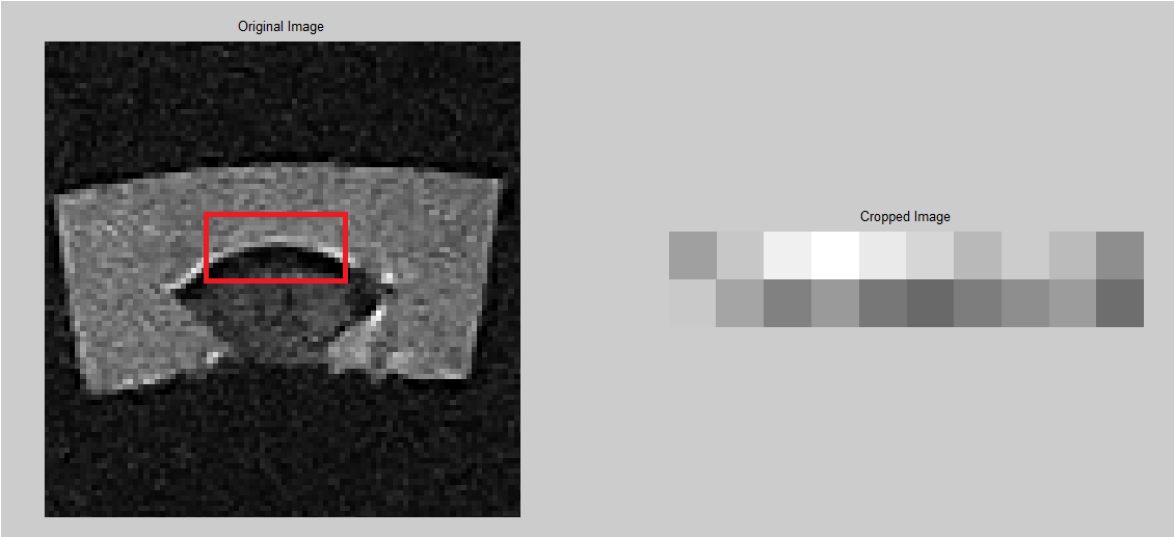

Figure 3.3: Grayscale of articular cartilage.

3.4 INDENTATION TEST

3.4.1 Apparatus

The equipment used to perform the indentation test and thickness test of articular cartilage is indentation test rig. The equipment consist of a shaft connected to a 4 mm diameter spherical indenter for creep test and a needle indenter for thickness test at its lower end. The indenters are shown in Figure 3.6. The movement of the shaft is detected by linear variable differential transformer (LVDT) that mounted on the top of the shaft. An analog-to-digital converter is used to process the data from LVDT and the data is stored in a computer using data acquisition software (LabVIEW 8.0, National Instruments Corporation, Austin, TX, USA.). The schematic diagram and indentation test rig are shown in Figure 3.4 and 3.5.

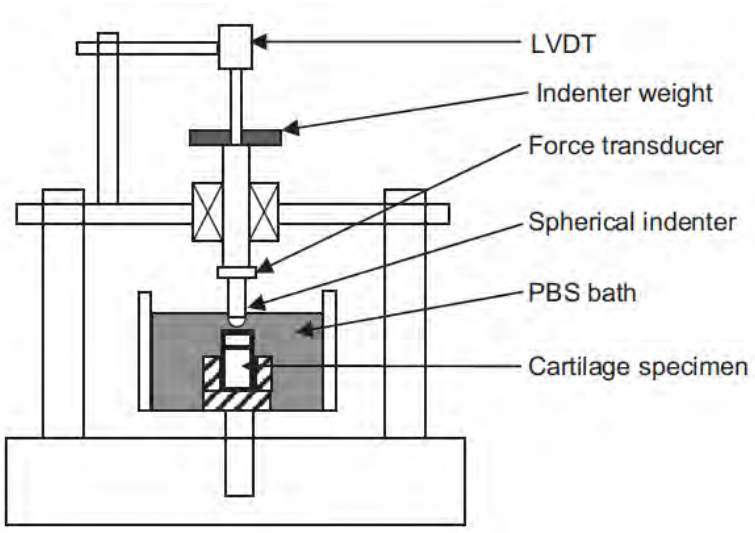

Figure 3.4: Schematic diagram of the indentation test rig.

Figure 3.5: Indentation test rig.

Figure 3.6: Indenters.

3.4.2 Calibration Procedure

Before performing the indentation test, calibration of the LVDT was conducted first. The purpose of calibration is to obtain the calibration factor for the displacement. The calibration factors were used to convert the voltage data to the actual distance and load generated from the LVDT during the indentation test. During the calibration, the LVDT represents the displacement and indenter represents the load have been connected to the transducer. The data from LVDT will transmitted to the computer.

The gauge blocks as shown in Figure 3. 7 are used to calibrate the LVDT. A total of six gauge blocks are used in this calibration test. The first test block is 4 mm and the increment of each block is start from 1.6 mm to 2.0 mm with 0.1 mm increment. During the test, the indenter is dropped on the block and deformation is recorded on the labview. After start the test, when the time reach 20 second, the indenter is released so that it touch the calibration block. The calibration test is performed for 1000 second and by the time, the displacement had reached equilibrium state. The average reading for each block is taken by perform the test 3 times. A graph of displacement versus transducer data was plotted by using the data obtained from the calibration test. The graph was plotted in a linear regression

fit of the voltage against the displacement which generate the linear equation as a calibration factor as shown in Figure 3.8.

Figure 3.7: Calibration gauge blocks.

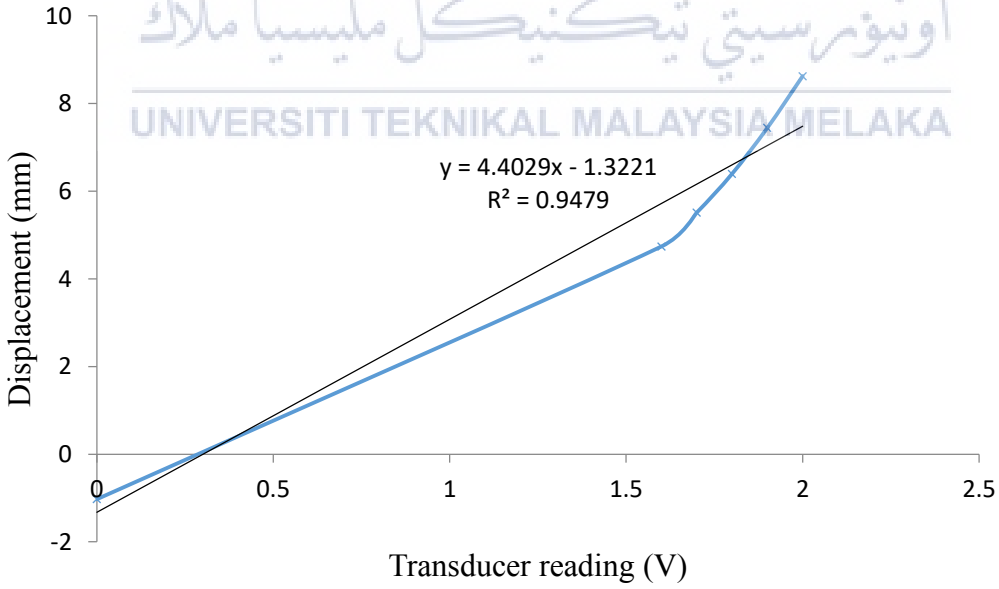

Figure 3.8: Graph of transducer data vs displacement.

The equation calculated from the graph will be used to find the deformation during the creep test. From the equation, y represent the displacement in voltage and x represent the displacement in millimeter. This equation is used to convert the displacement in voltage obtain from LVDT to displacement in millimeter.

3.4.3 Creep Compression Test

For the indentation test, creep compression test were carried out in order to provide experiment data to characterize the biphasic properties of the cartilage. The test was carried out using a 4 mm diameter spherical indenter subjected to 0.38 N compression force. Besides, the test was conducted using four specimens of cow articular cartilage. The cartilage is submerged in PBS solution throughout the test to ensure that the cartilage always in hydrated condition. The indenter was placed close to the cartilage surface by monitoring the load indicator. The reason for this act is to prevent the additional force subject to the cartilage surface when dropping the indenter onto the cartilage surface. After the test is run for 20 second, the indenter was released. Then, the test was run for 2000 seconds until the displacement had reached the equilibrium state. The displacement and load readings were recorded at a frequency of 0.1s. The result of creep compression curve is as shown in Figure 3.9.

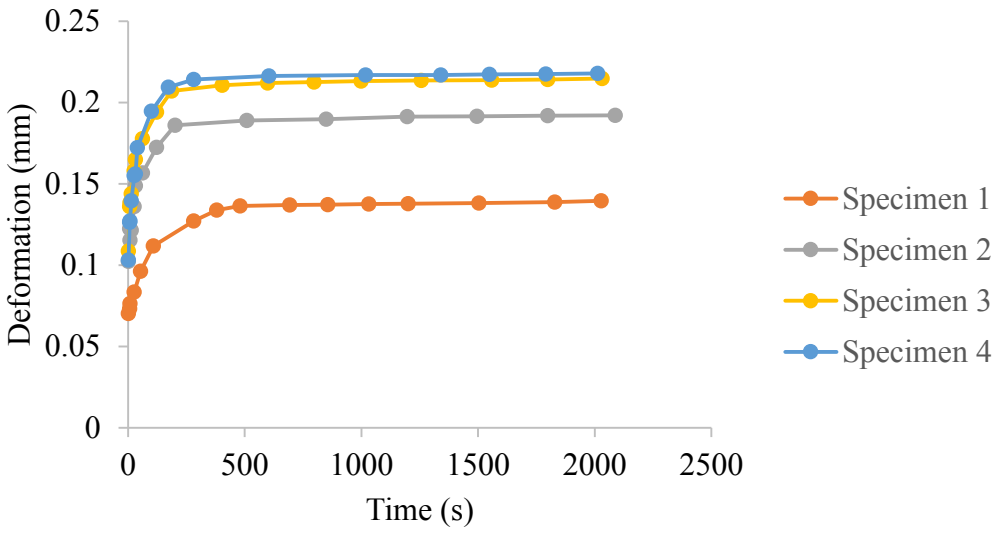

Figure 3.9: Creep indentation test result for 1st sample.

3.4.4 Thickness Test

Beside the creep test, indentation test also used to measure the thickness of cartilage. The cartilage thickness was measured using a needle indenter and with a load of 3.18 N. In order to obtain accurate data, the displacement and load readings were recorded at the frequency of 0.001s. The thickness of the cartilage is the difference between the position of the needle when it contacted the cartilage surface and when it contacted the bone (Latif, et al, 2012). As the test is started, the indenter is straight away released. The test was stopped as long as the indenter touch the bone. A graph is plotted by using the data obtain from the thickness test. Again, the equation generates from the calibration test is used to convert the displacement data from voltage into millimeter in order to calculate the thickness. The thickness result obtain in indentation test will be used in the FE modelling of articular cartilage.

3.5 RADIUS MEASUREMENT OF THE CARTILAGE

The radius of the cartilage was measured by using profile projector. The specimen was put on top of the stage. The curvature surface is facing upward and 10 points from the curvature surface was marked down by adjust the stage to move in the horizontal and vertical direction. After the 10 points was marked, the reading is recorded. This process was repeat for another two times to get the average value. All the four specimens' radius were recorded. The Figure 3.10 shows the profile projector used to obtain the radius of the curvature.

Figure 3.10: Profile projector

3.6 FINITE ELEMENT MODELLING

An axisymmetric biphasic finite element model was generate to simulate the creep indentation test experiment on the cartilage specimen. The specimen was modelled according to the real cartilage specimen including the thickness and curvature of the articular

cartilage. The specimen was modelled at a constant 1.9 mm height. Besides, the spherical indenter with 4mm diameter was modelled as an analytical rigid body. All the 4 specimens are drawn as quarter part of the whole femoral head. An example of the FE model is shown in Figure 3.11.

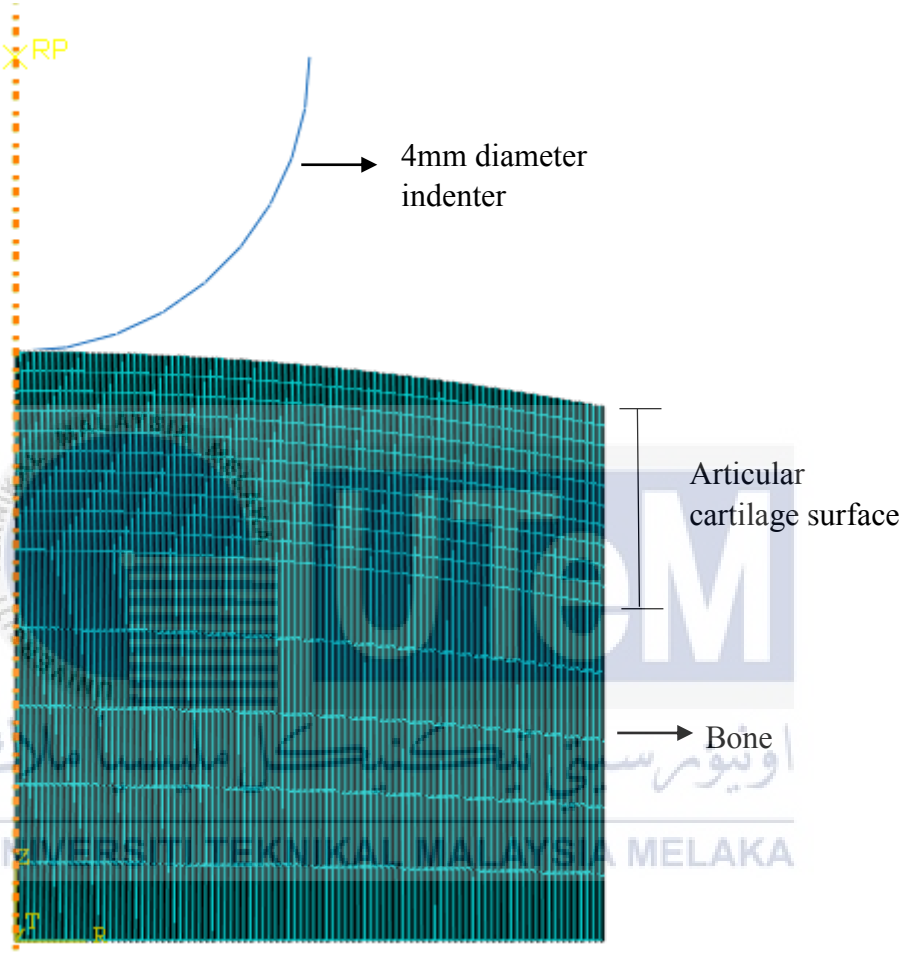

Figure 3.11: Finite element modelling of articular cartilage.

The bottom nodes were constrained in both horizontal and vertical direction while the nodes on the axis were constrained in the horizontal direction. Besides, the spherical indenter was restricted only can move in vertical direction. This steps were done in order to meet the actual experimental conditions so that the curve produced is same as the experimental curve.

Furthermore, mesh sensitivity analysis was also implemented to the specimen model in order to optimise the result. The mesh density of the specimen divided into two part, articular cartilage and bone. For the cartilage part, the mesh density consist of 2000 (200 x 10 in the horizontal and vertical directions respectively) elements, and for bone, the mesh density consist of 1000 (200 x 5 in the horizontal and vertical directions respectively) elements as shown in Figure 3.10.

3.7 CHARACTERIZATION OF BIOMECHANICAL PROPERTIES

The finite element (FE) models were used to determine the elastic modulus and permeability of articular cartilage by using curve fitting technique. The experimental result produce a curve similar to the curve generated by FE models. Then, the experimental curve was fit to the FE model's curve in order to determine the biomechanical properties by using Microsoft Visual Studio and MATLAB. The curve fitting process is shown in Figure 3.12.

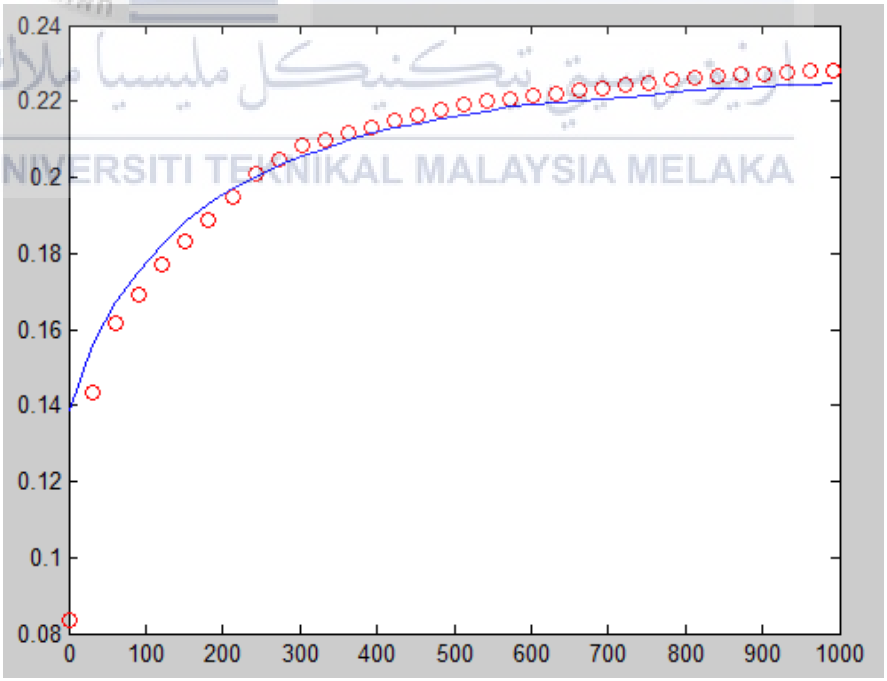

Figure 3.12: Curve fitting of both indentation creep test curve and FE model curve.

The blue curve indicates the FE model generated curve whereas the red dot curve indicates the indentation creep test curve. The blue curve is slowly fit to the red curve in order to get the biomechanical properties of articular cartilage.

3.8 CORRELATION OF MRI GRAYSCALE AND BIOMECHNICAL PROPERTIES OF ARTICULAR CARTILAGE

The correlation between MRI grayscale and biomechanical properties also been made by using Linear Pearson Correlation method. This correlation is the measure of the linear correlation between two variables, in this study, the variables are MRI grayscale and biomechanical properties. The Pearson correlation coefficient has a value between +1 and -1, which indicate that positive and negative linear correlation respectively and 0 indicates no linear correlation. The correlation result is discussed in chapter 4.

CHAPTER 4

RESULTS AND DISCUSSIONS

4.1 INTRODUCTION

This chapter discuss the result of the experiment. The results include the selection of MRI sequence, determination of articular cartilage grayscale, FE modelling of articular cartilage in finding the biomechanical properties of articular cartilage, and the correlation between the biomechanical properties and grayscale value.

4.2 SELECTION OF MRI SEQUENCE

There are a total of five sequences used in the MRI scanning of the articular cartilage. The sequences used are shown in Table 4.1. The transverse plane scanning was used for all five sequences because it shows the most suitable position and orientation of articular cartilage.

Table 4.1: Sequences used in MRI scanning.

Gradient echo	Gradient echo STIR	Spin echo T1
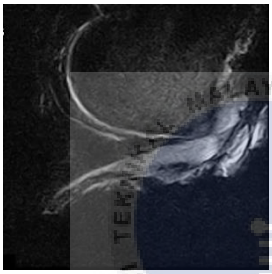		

Spin echo T2	Turbo spin echo
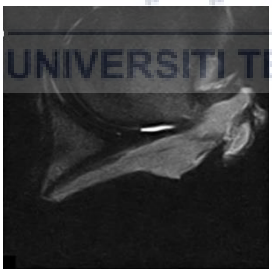	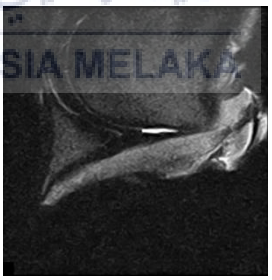

By visually, from the five sequences, spin echo T1 shows that highest contrast and most clear image compare to other four sequences. Therefore, the best sequence chooses for the characterization of the grayscale was spin echo T1. In terms of grayscale, spin echo T1 has the grayscale range of 1327 to 1805 and have the average value of 1531, which is greater

than the other sequences. This sequence was also used in previous study to investigate the articular cartilage (Damion, et al., 2012).

From the grayscale image in Figure 3.3 (chapter 3), it consists of two layer. The outer layer represents the fluid phase of articular cartilage, whereas the second layer represents the solid phase. The grayscale value of these two layer have some difference, as shown in Figure 4.1.

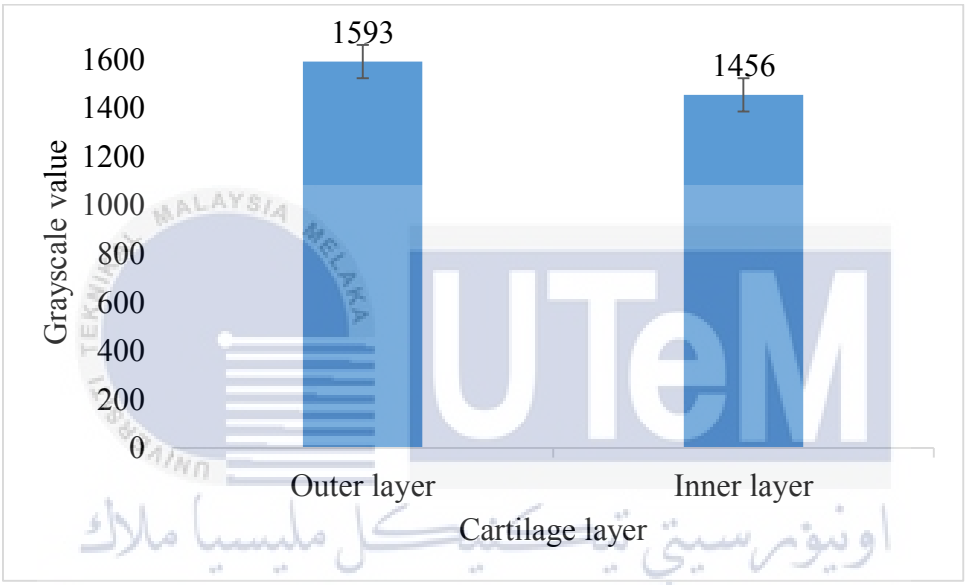

Figure 4.1: The grayscale value of cartilage layer.

For the outer layer, it has high grayscale value compare to inner layer. This is due to the outer layer is made of fluid, or in other words, it is fluid phase. The two layer of the articular cartilage shows that it is a biphasic material.

4.3 THICKNESS TEST RESULT FROM INDENTATION TEST

The thickness test results were used to create the FE model of articular cartilage so that the model is close to the real sample. The radius and thickness of each specimen were used to create the coordinates in FE modelling. The thickness result is shown in Figure 4.2.

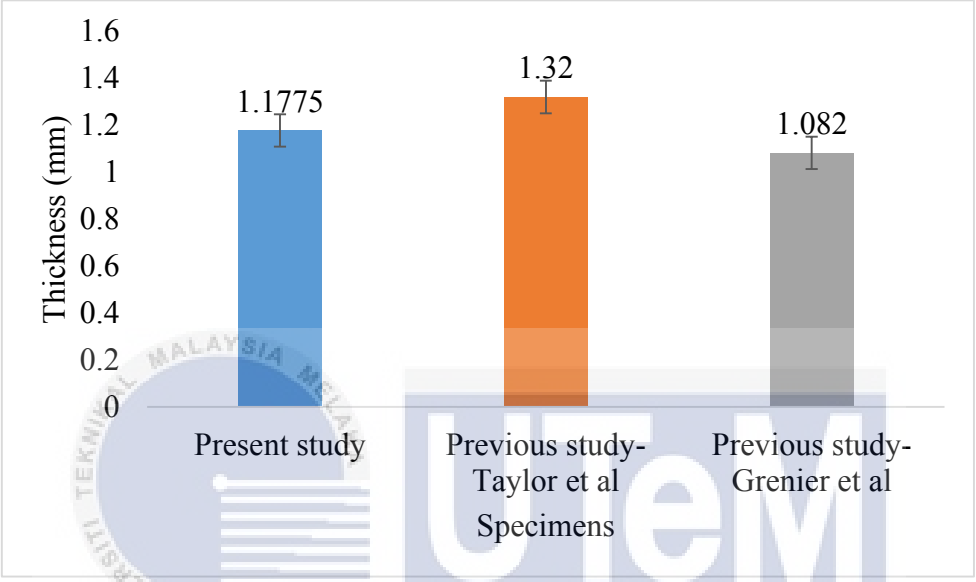

Figure 4.2: Thickness of articular cartilage.

4.4 BIOMECHANICAL PROPERTIES OF ARTICULAR CARTILAGE

After the curve fitting process is done, the biomechanical properties of articular cartilage is obtained as shown in Figure 4.3 and Figure 4.4. The biomechanical properties for the present study are the average value of eight specimens.

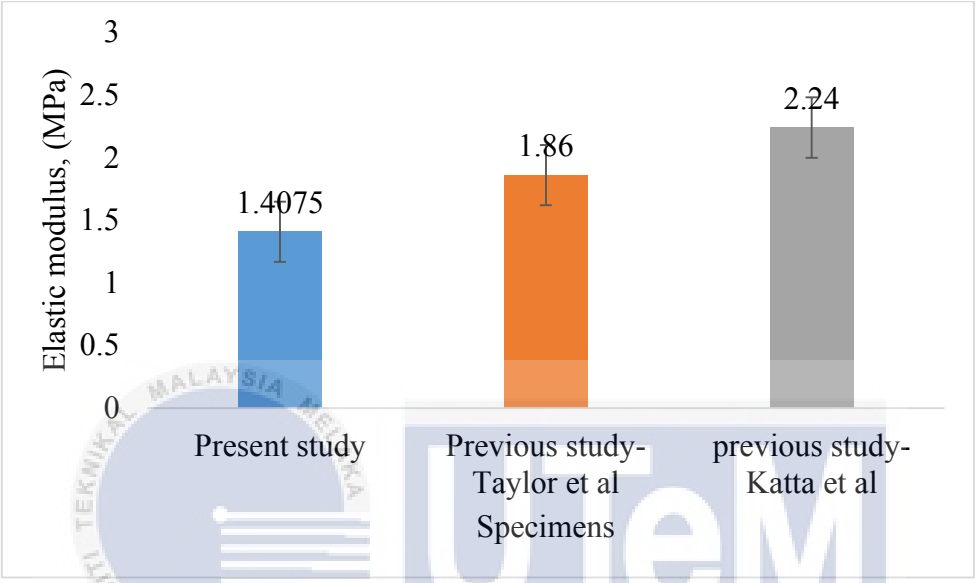

Figure 4.3: Elastic modulus of articular cartilage.

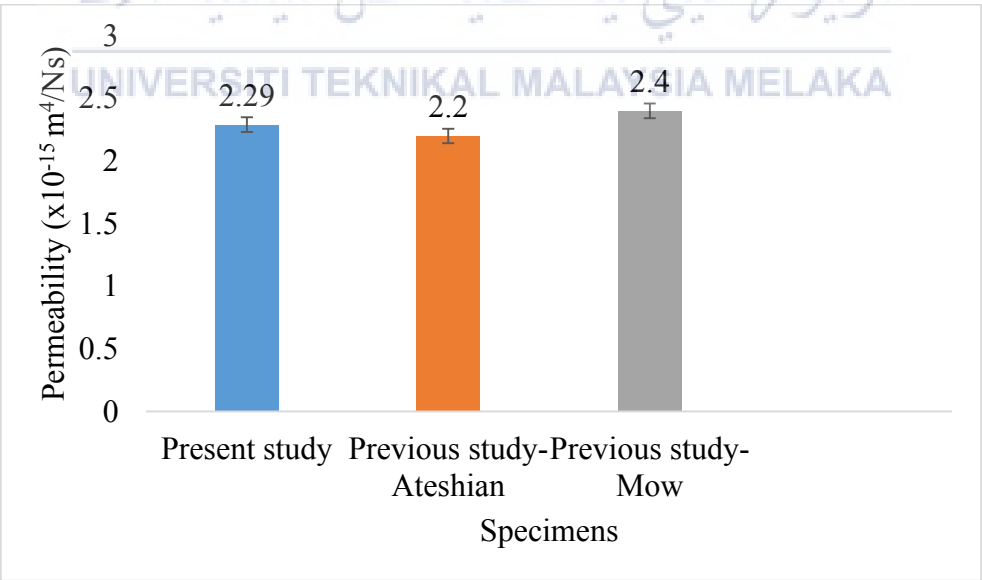

Figure 4.4: Permeability of articular cartilage.

4.4.1 Linear Pearson Correlation of Biomechanical Properties

Linear Pearson correlation is used to measure the linear correlation between 2 variables. In this case, it is used to correlate the grayscale value and the biomechanical properties (elastic modulus and permeability). From the correlation as shown in Figure 4.5 and 4.6, the r value for both result are 0.5416 and 0.6877. These value is exceed 0.5 which means that the grayscale value have a significant effect on the biomechanical properties. As the r value approach to 1, the higher the correlation between the grayscale and biomechanical properties.

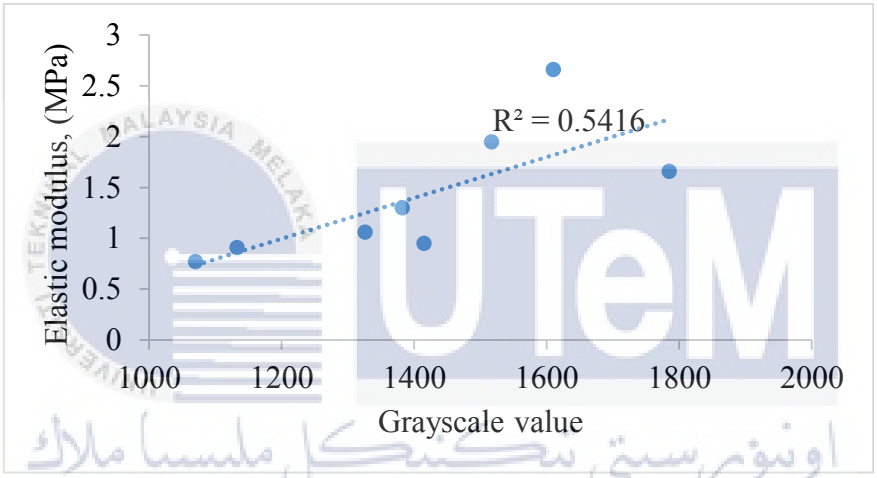

Figure 4.5: Correlation between elastic modulus and grayscale value of articular cartilage.

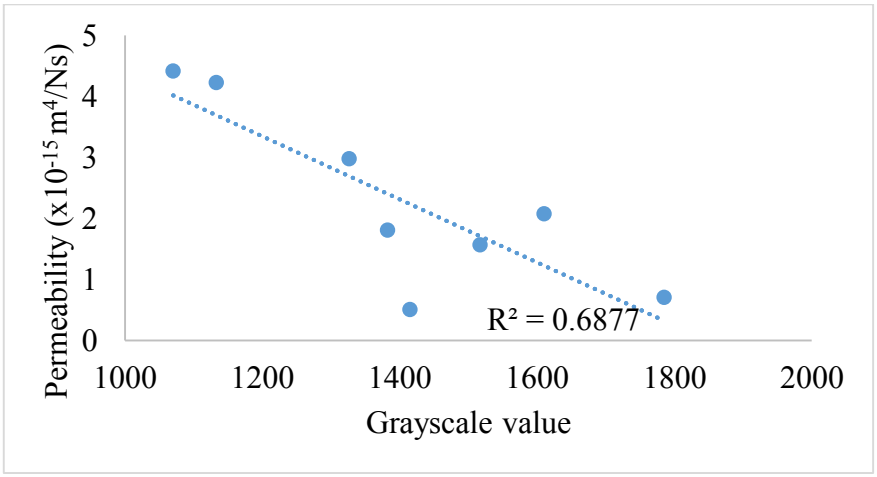

Figure 4.6: Correlation between permeability and grayscale value of articular cartilage.

4.5 DISCUSSION

This study has provided the method to characterize the biomechanical properties of bovine articular cartilage by using the combination of experimental and computational method. The methods included in characterize the biomechanical properties are MR Imaging (MRI), indentation test and FE modelling of articular cartilage. Besides, the correlation between the grayscale value from MRI and biomechanical properties (elastic modulus and permeability) were also determine. In this study, the bovine hip joint was used to carry out the experiment. In most of the study of articular cartilage, animal models are widely used due to its physiological and metabolic factor. Animal models also have proper long-term transient changes in tissue structure and joint organization (Grenier, Bhargava, & Torzilli, 2014). Besides, animal model also easily to obtain compare to human joint.

There are few sequences used in MRI and the highest contrast image is chosen and used to characterize the biomechanical properties. From the grayscale value, the relationship between the biomechanical properties and grayscale value can be correlate by linear pearson correlation. If the correlation factor, $\rho > 0.5$, the grayscale values have a significant effect on the biomechanical properties.

Other than MRI method, indentation test was also carried out to characterize the biomechanical properties of articular cartilage. Indentation test is widely used to determine the biphasic properties of articular cartilage in previous and current study. Basically, there two types of indentation, which are creep test and thickness test. Creep indentation test is used to obtain the equilibrium curve and the curve is used in the curve fitting process. For thickness test, the thickness was obtain in order to create the FE model. The FE model was created according to the dimension of the real sample. An axisymmetric biphasic poroelastic

model was created to characterize the elastic modulus and permeability of articular cartilage. This FE model is then match the cartilage deformation that was generated from the creep test by using MATLAB.

The biomechanical properties obtained from the FE model were used to compare with the previous study. Both the elastic modulus and permeability result are closed to the previous study and it is an acceptable results. Besides, the Linear Pearson correlation between the MRI grayscale and biomechanical properties also been make. The r value for both elastic modulus and permeability were exceeded 0.5.This shows that the grayscale values have an important effect on the biomechanical properties.

There are some important issues need to be consider for the sample preparation and the indentation test. The sample preparation, MRI scanning and the indentation test must be done in 48 hours in order to maintain the freshness of articular cartilage. This provide the best articular cartilage surface for the indentation test. Before the specimens store in the fridge, it is soak with PBS (Phosphate Buffered Saline) solution so that to make the articular surface hydrated. During the indentation test, the specimens is fully submerged in PBS in order to keep the articular surface hydrated. Furthermore, the specimens must fit tightly inside the specimen holder and not allow to move during the indentation test so that it will not affect the results. Besides, the indenter was placed close to the cartilage surface so that no external force is created.

CHAPTER 5

CONCLUSION

5.1 CONCLUSION

Osteoarthritis (OA) is a joint disease that results from the breakdown of joint cartilage. This disease will limit the movement of human and affect the daily life of a person. The main purpose of this study is to estimate the biomechanical properties of articular cartilage by using a slaughter cow's hip joint. From previous study, extensive experimental and computational studies have been performed to characterize the biomechanical properties of articular cartilage. In this study, the same approach was used to characterize the biomechanical properties of articular cartilage. In order to study the articular cartilage, the behavior of articular cartilage must be known beforehand to solve the degeneration of articular cartilage of human. Hence, the animal articular cartilage was used to study the behavior of cartilage. First of all, the specimens was scanned using MRI and the clearest image was chosen to obtain the grayscale value. The biomechanical properties of articular cartilage were obtained through the combination of both experimental and computational method. From the study, the elastic modulus and permeability of bovine articular cartilage are 1.4075 MPa and 2.29 x 10^{-15} m^4/Ns respectively, which were closed to the previous study. After that, a correlation was made between the MRI grayscale value and biomechanical properties. From this correlation, it can be conclude that the MRI grayscale play a significant effect on the biomechanical properties.

REFERENCES

A Chen, C. G. (2012). The global economic cost of osteoarthritis: how the UK compares. *Arthritis*.

Braun, H. J., & Gold, G. E. (2012). Diagnosis of osteoarthritis: Imaging. *Bone*, 278-288.

Burgkart, R., Glaser, C., Hyhlik-Du¨rr, A., Englmeier, K.-H., Reiser, M., & Eckstein, F. (2001). Magnetic resonance imaging–based assessment of cartilage loss in severe osteoarthritis. *Arthritis & Rheumatism*, *44(9)*, 2072-2077.

Damion, R., Pawaskar, S., Ries, M., Ingham, E., Williams, S., Jin, Z., & Radjenovic, A. (2012). Spine-lattice relaxation rates and water content of freeze-dried articular cartilage. *Osteoarthritis and Cartilage*,*20(2)*, 184-190.

Eckstein, F., Cicuttini, F., Raynauld, J.-P., Waterton, J. C., & Peterfy, C. (2006). Magnetic resonance imaging (MRI) of articular cartilage in knee. *Osteoarthritis and Cartilage*, 46-75.

Fox, A. J., Bedi, A., & Rodeo, S. A. (2009). The basic science of articular cartilage: structure, composition, and function. *Sports Health: A Multidisciplinary Approach*, 461-468.

Fransen, M., Bridgett, L., March, L., Hoy, D., Penserga, E., & Brooks, P. (2011). The epidemiology of osteoarthritis in Asia. *International journal of rheumatic diseases*, 113-121.

Goldy, G. E., Bursteinz, D., Dardzinskix, B., Lang, P., Boada, F., & Mosher, T. (2006). MRI of articular cartilage in OA: novel pulse sequences and compositional/functional markers. *Osteoarthritis and Cartilage, 14*, 76-86.

Grenier, S., Bhargava, M. M., & Torzilli, P. A. (2014). An in vitro model for the pathological degradation of articular cartilage. *Journal of biomechanics, 47(3)*, 645-652.

Hani, A. F. M., Malik, A. S., Kumar, D., Kamil, R., Razak, R., & Kiflie, A. (2011, July). Features and modalities for assessing early knee osteoarthritis. In *Electrical Engineering and Informatics (ICEEI), 2011 International Conference on* (pp. 1-6). IEEE.

Hashim, N. H., Latif, M. J. A., & Jaafar, Y. L. (2015, March). The effects of contact area and surface curvature on biomechanical behavior of articular cartilage. In *Biomedical Engineering (ICoBE), 2015 2nd International Conference on* (pp. 1-4). IEEE.

Heyden, R. J. (2016). *Anatomy & Physiology.* Texas: OpenStax.

Johnson, V. L., & Hunter, D. J. (2014). The epidemiology of osteoarthritis. *Best practice & research clinical rheumatology, 28(1)*, 5-15.

Juras, V., Bittsansky, M., Majdisova, Z., Szomolanyi, P., Sulzbacher, I., Gäbler, S., . . . Trattnig, S. (2009). In vitro determination of biomechanical properties of human articular cartilage in osteoarthritis using multi-parametric MRI. *Journal of Magnetic Resonance197(1)*, 40-47.

Kapoor, M., & Mahomed, N. N. (Eds.). (2015). *Osteoarthritis: Pathogenesis, diagnosis, available treatments, drug safety, regenerative and precision medicine.* Springer.

Katta, J., Pawaskar, S. S., ZMJin, Ingham, E., & Fisher, J. (2007). Effect of load variation on the friction properties of articular cartilage. *Proceedings of the Institution of Mechanical Engineers, Part J: Journal of Engineering Tribology*, *221*(3), 175-181.

Kinsella, K., & He, W. (2009). *An aging world: 2008: International population reports*. US Government Printing Office.

Kubakaddi, S., Ravikumar, K. M., & Harini, D. G. (2013, January). Measurement of cartilage thickness for early detection of knee osteoarthritis (KOA). In *Point-of-Care Healthcare Technologies (PHT), 2013 IEEE* (pp. 208-211). IEEE.

Latif, M. J. (2011). *Characterisation and Modelling of Spinal Facet Joints.* The University of Leeds.

Latif, M. J., Hashima, N. H., Ramlana, R., Mahmudc, J., Jumahatc, A., & Kadird, M. R. (2013). The Effects of Surface Curvature on Cartilage Behaviour in Indentation Test: A Finite Element Study. *Procedia Engineering, 68*, 109-115.

Latif, M. J., Jin, Z., & Wilcox, R. K. (2012). Biomechanical characterisation of ovine spinal facet joint cartilage. *Journal of biomechanics, 45(8)*, 1346-1352.

Lawrence, C., Felson, D. T., Helmick, C. G., Arnold, L. M., Choi, H., Deyo, R. A., . . . Wolfe, F. (2008). Estimates of the prevalence of arthritis and other rheumatic conditions in the United States: Part II. *Arthritis & Rheumatism, 58(1)*, 26-35.

Li, L. P., Herzog, W., Korhonen, R. K., & Jurvelin, J. S. (2005). The role of viscoelasticity of collagen fibers in articular cartilage: axial tension versus compression. *Medical engineering & physics*, *27*(1), 51-57.

Lu, X. L., & Mow, V. C. (2008). Biomechanics of articular cartilage and determination of material properties. *Medicine & Science in Sports & Exercise, 40(2)*, 193-199.

Magee, T., Shapiro, M., & Williams, D. (2003). Comparison of high-field-strength versus low-field-strength MRI of the shoulder. *American Journal of Roentgenology*, *181*(5), 1211-1215.

Mansour, J. M. (2009). Biomechanics of Cartilage. In C. A. Oatis, *Kinesiology: The Mechanics and Pathomechanics of Human Movement* (pp. 69-83). Philadelphia: Lippincott Williams & Wilkins.

McMahon, K. L., Cowin, G., & Galloway, G. (2011). Magnetic resonance imaging: the underlying principles. *journal of orthopaedic & sports physical therapy*, *41*(11), 806-819.

Messier, S. P., Legault, C., Mihalko, S., Miller, G. D., Loeser, R. F., DeVita, P., . . . Nicklas, B. J. (2009). The Intensive Diet and Exercise for Arthritis (IDEA) trial: design and rationale. *BMC musculoskeletal disorders, 10(1),* 1.

Michael, J. W., Schlüter-Brust, K. U., & Eysel, P. (2010). The epidemiology, etiology, diagnosis, and treatment of osteoarthritis of the knee. *Dtsch Arztebl Int*, *107*(9), 152-62.

Palazzo, C., Christelle Nguyen, M.-M. L.-C., Rannou, F., & Poiraudeau, S. (2016). Risk factors and burden of osteoarthritis. *Annals of physical and rehabilitation Medicine*, 134-138.

Poole, A. R., Kojima, T., Yasuda, T., Mwale, F., Kobayashi, M., & Laverty, S. (2001). Composition and structure of articular cartilage: a template for tissue repair. *Cliniacal orthopaedics and related research, 391*, S26-S33.

Pujol, E., Van Bree, H., Cauzinille, L., Poncet, C., Gielen, I., & Bouvy, B. (2011). Anatomic Study of the Canine Stifle Using Low-Field Magnetic Resonance Imaging (MRI) and MRI Arthrography. *Veterinary Surgery*, *40*(4), 395-401.

Schrauth, J. H., Lykowsky, G., Hemberger, K., Kreutner, J., Weber, D., Rackwitz, L., ... & Haddad, D. (2015). Comparison of multiple quantitative MRI parameters for characterization of the goat cartilage in an ongoing osteoarthritis: dGEMRIC, T 1ρ and sodium. *Zeitschrift für Medizinische Physik*.

Shepherd, D. E., & Seedhom, B. B. (1999). Thickness of human articular cartilage in joints of the lower limb. *Annals of the rheumatic diseases, 58(1)*, 27-34.

Simon, W. H. (1970). Scale effects in animal joints. I. Articular cartilage thickness and compressive stress. *Arthritis and Rheumatism, 13(3)*, 244-256.

Sinusas, K. (2012). Osteoarthritis: Diagnosis and Treatment. *American family physician 85(1)*, 49-56.

Soh, S. S., Swee, T. T., Ying, S. S., En, C. Z., bin Mazenan, M. N., & Meng, L. K. (2014, November). Magnetic resonance image segmentation for knee osteoarthritis using active shape models. In *Biomedical Engineering International Conference (BMEiCON), 2014 7th* (pp. 1-5). IEEE

Spector, T. D., & MacGregor, A. J. (2004). Risk factors for osteoarthritis: genetics. *OsteoArthritis and Cartilage, 12*, 39-44.

Taruc-Uy, R. L., & Lynch, S. A. (2013). Diagnosis and treatment of osteoarthritis. *Primary Care: Clinics in Office Practice, 40(4)*, 821-836.

Taylor, S. D., Tsiridis, E., Ingham, E., Jin, Z., Fisher, J., & Williams, S. (2011). Comparison of human and animal femoral head chondral properties and geometries. *Journal of Engineering in Medicine*, 55-62.

Vignon, É., Valat, J.-P., Rossignol, M., Avouac, B., Rozenberg, S., Thoumie, P., . . . Hilliquin, P. (2006). Osteoarthritis of the knee and hip and activity: a systematic international review and synthesis (OASIS). *Joint Bone Spine, 73(4)*, 442-455.

Wang, C. C.-B., Deng, J.-M., Ateshian, G. A., & Hung, C. T. (2002). An automated approach for direct measurement of two-dimensional strain distributions within articular cartilage under unconfined compression. *Journal of Biomechanical Engineering, 124(5)*, 557-567.

APPENDIX A1 Creep test raw data (sample 1)

Specimen 1

Time	Deformation
2	0.07020373
6.8	0.073088192
8	0.076267915
26	0.083490427
54.3	0.096186605
109.2	0.111789957
281.7	0.12709805
479.8	0.136341957
692.4	0.136932477
1031.9	0.137500284
1200	0.137795544
1503.8	0.138090804
1829.3	0.138658612
2027.8	0.139521679

Specimen2

Time	Deformation
6.6	0.122487451
9	0.115264939
14	0.121329124
26	0.136069409
32	0.148765586
62	0.156578618
122	0.172454518
201.8	0.186036476
508.7	0.188920938
849.8	0.189806718
1196.5	0.191237593
1494.9	0.191532853
1799.3	0.191828113
2087.7	0.192100661

Specimen 3

Time	Deformation
2	0.108632946
8	0.138386064
14	0.143882441
26	0.158032206
32	0.164959458
62	0.177678348
122	0.194144768
187	0.207136205
404.2	0.210611188
599	0.212064775
998.8	0.213223103
1257.2	0.21349565
1559.3	0.21379091
2032.3	0.214653978

Specimen 4

Time	Deformation
2	0.103136569
8	0.127120762
14	0.139544392
26	0.155147744
32	0.156010811
40	0.172181971
100.3	0.194735288
173	0.209452861
282	0.214086171
603.4	0.216402826
1340.9	0.216970633
1549.2	0.217265893
1790	0.217538441
2012.5	0.217833701

APPENDIX A2 Creep test raw data (sample 2)

Specimen 1

Time	Deformation
2	0.032158734
6.8	0.053958155
32	0.098556222
62	0.130980057
122	0.164443901
302	0.205697623
591.4	0.23137159
1003.1	0.245890942
1230.7	0.25082589
1449.1	0.25290591
1791.4	0.256780456
1910.8	0.257045557
2060.8	0.258350667

Specimen 2

Time	Deformation
2	0.037093682
8	0.056282882
14	0.063542559
32	0.090786737
62	0.10453118
122	0.122435662
302	0.147069619
523.2	0.153819487
899.6	0.157449325
1200.2	0.158999143
1696.7	0.160304254
1909.2	0.161079163
2054.7	0.161588972

Specimen 3

Time	Deformation
2	0.083527061
6.8	0.10479628
8	0.107651209
14	0.123740772
26	0.135140095
32	0.143460174
62	0.161609364
122	0.176903626
242	0.201027774
500	0.218932257
808.7	0.226191933
1300.8	0.230861781
1523.6	0.232411599
1900	0.234491619
2045.7	0.235266528

Specimen 4

Time	Deformation
2	0.049023206
6.8	0.076512092
14	0.10037114
32	0.12398548
62	0.156144214
122	0.187262938
200	0.217606753
302	0.236551245
602	0.264570333
1002	0.277784575
1230	0.283249724
1500	0.285574452
1680	0.286614462
1796.8	0.287654472
2057.2	0.28893919

APPENDIX A3 Example of thickness test graph

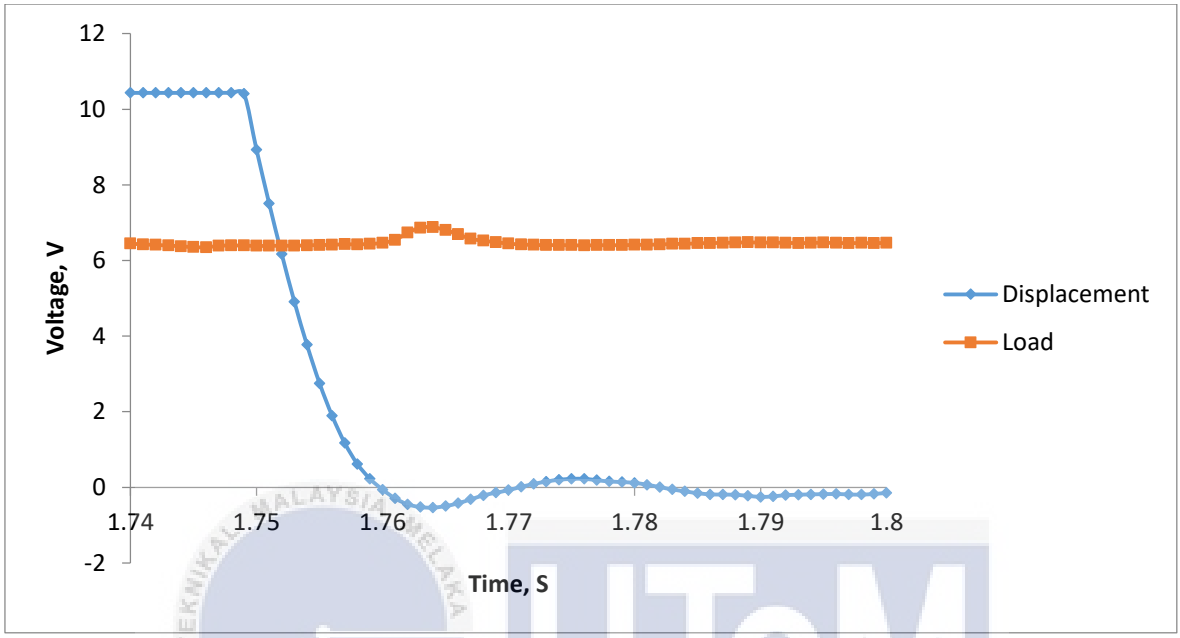

APPENDIX B1 Coordinate of FE modelling (1st sample)

Sample curvature radius

Specimens	1	2	3	Average
1	21.545	21.725	21.819	21.696
2	21.556	21.895	21.132	21.528
3	20.906	21.245	21.284	21.163
4	21.052	20.899	20.499	20.817

thickness result

Specimens	Thickness
1	1.3477
2	1.5223
3	1.3633
4	1.0221

FE modelling

Curve trimming points; Start point = (0, -radius +4); end point = (0,4)

Specimens	(x,y)
1	(-1.97, 2.06)
2	(-1.97, 2.06)
3	(-1.97, 2.06)
4	(-1.97, 2.06)

Specimens	Start point	End point
1	(0, -17.70)	(0,4)
2	(0, -17.53)	(0,4)
3	(0, -17.16)	(0,4)
4	(0, -16.82)	(0,4)

Partition coordinates; centre point = (x, y-thickness-radius); end point = x, y-thickness)

Specimens	Centre point	End point	Node value
1	(-1.97, -20.98)	(-1.97, 0.71)	7
2	(-1.97, -20.99)	(-1.97,0.54)	6
3	(-1.97, -20.47)	(-1.97, 0.70)	6
4	(-1.97, -19.78)	(-1.97, 1.04)	6

APPENDIX B2 Coordinate of FE modelling (2nd sample)

Sample curvature radius

Specimens	1	2	3	Average
1	22.046	22.859	21.965	22.29
2	20.992	20.49	19.136	20.206
3	21.97	22.611	21.686	22.089
4	21.159	21.154	20.739	21.01733333

Thickness result

Specimens	Thickness
1	1.049
2	1.031
3	0.937
4	1.151

FE modelling

Curve trimming points; Start point = (0, -radius +4); end point = (0,4)

Specimens	(x,y)
1	(-1.97, 2.06)
2	(-1.97, 2.06)
3	(-1.97, 2.06)
4	(-1.97, 2.06)

Specimens	Start point	End point
1	(0, -18.29)	(0,4)
2	(0, -16.21)	(0,4)
3	(0, -18.09)	(0,4)
4	(0, -17.02)	(0,4)

Partition coordinates; centre point = (x, y-thickness-radius); end point = x, y-thickness)

Specimens	Centre point	End point	Node value
1	(-1.97, -21.28)	(-1.97, 1.01)	6
2	(-1.97, -19.18)	(-1.97,1.02)	6
3	(-1.97, -20.97)	(-1.97, 1.12)	7
4	(-1.97, -20.11)	(-1.97, 0.91)	6